

Centrifuge modelling of temporary roadway systems subject to rolling type loading

Andrew S. Lees*¹ and David J. Richards²

¹*Frederick University, Nicosia, Cyprus and Geofem Ltd., Cyprus*

²*University of Southampton, Southampton, UK*

(Received June 17, 2010, Accepted February 21, 2011)

Abstract. Scaled centrifuge modelling techniques were used to study the soil-structure interactions and performance of a jointed rollable aluminium roadway (or trackway) system on soft clay under light truck tyre loads. The measured performance and subsequent analyses highlighted that the articulated connections significantly reduced the overall longitudinal flexural stiffness of the roadway leading to stress concentrations in the soil below the joints under tyred vehicle loadings. This resulted in rapid localised failure of the supporting soil that in turn led to excessive transverse flexure of the roadway and ultimately plastic deformations. It is shown that the performance of rollable roadway systems under tyred vehicle trafficking will be improved by eliminating joint rotation to increase longitudinal stiffness.

Keywords: model tests; tyre; clay; rutting; roadway; trackway; soil-structure interaction; centrifuge modelling.

1. Introduction

Temporary roadway systems are often used to provide continued vehicle access over soft ground encountered at rural locations or increasingly, at public events necessitating parking on unpaved areas. There are many forms of proprietary roadway systems (Perry and Myers 1984, Arciszewski and Wiedeck 1987, Glaza *et al.* 1994, Davis and Davis 2004). For civilian applications these tend to comprise stiff panels or mats fabricated from either aluminium or composite materials that are laid on the ground where heavy trafficking is expected. These temporary roadway systems may be individually anchored to the ground or inter-connected using articulated joints requiring a separate connection operation for each panel to form a continuous roadway (Fig. 1).

Military trackway systems are similar but generally of heavier duty and designed to be rapidly deployed and retrieved. One such system involves a roadway (or trackway) comprising corrugated aluminium panel extrusions (Fig. 2) each connected by a series of articulated joints. This allows the roadway to be unrolled directly onto the ground from lorry-mounted spools and re-rolled back onto the spools for rapid retrieval. These temporary roadway systems are used by both tracked and tyred vehicles. However, the transfer of repeated loading to the underlying ground through the roadway system from tyred vehicles has been seen to lead to localised rutting (as defined in Fig. 3) and

*Corresponding author, Ph.D., E-mail: Andrew.Lees@geofem.net

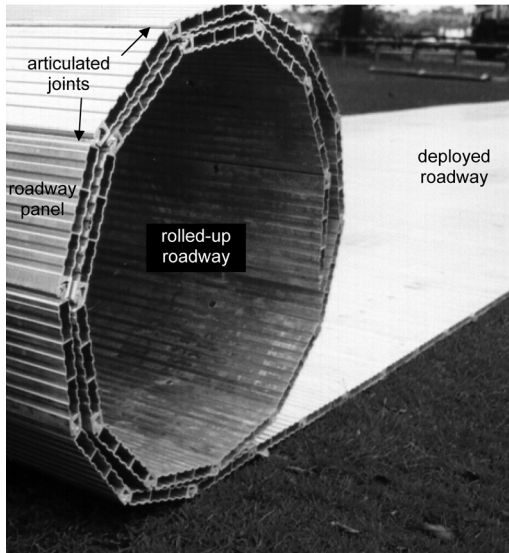


Fig. 1 Deployment of rollable aluminium roadway
(Courtesy: Eve Trakway Ltd.)



Fig. 2 Extruded aluminium section of Class 60 trackway panel

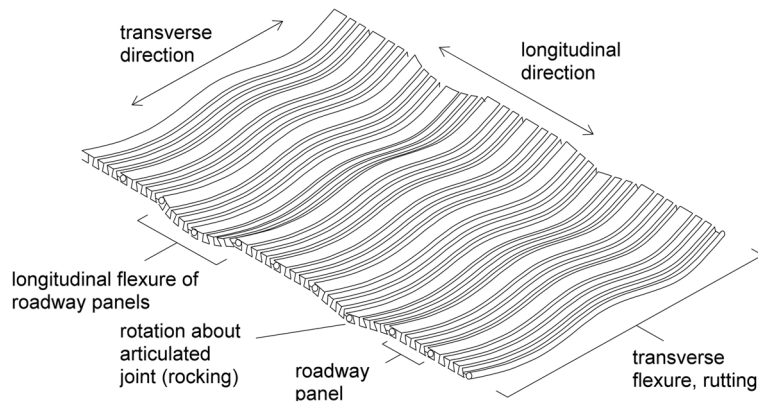


Fig. 3 Roadway labelling convention

permanent plastic deformation of the roadway system due to a loss of stiffness in the underlying ground. These deformations hinder the continued progress of vehicles and also retrieval of the roadway since panel deformations restrict normal operation of the joints preventing the roadway from being rolled back onto the vehicle mounted spools.

It is known from field experience and studies related to landing mat systems (Georgiadis 1979, Butterfield and Georgiadis 1980a, 1980b) that roadway deformations (rutting) accumulate due to successive vehicle passes rather than due to a single heavy vehicle loading event. However, the precise mechanisms of roadway rutting are poorly understood, due in part to a paucity of research in this field. While there are several established texts on the interactions between flexible foundations and the ground such as Poulos and Davis (1974), Hemsley (1998) and Selvadurai (1979), these are elastic analyses and are unable to accommodate permanent deformations. Bearing capacity

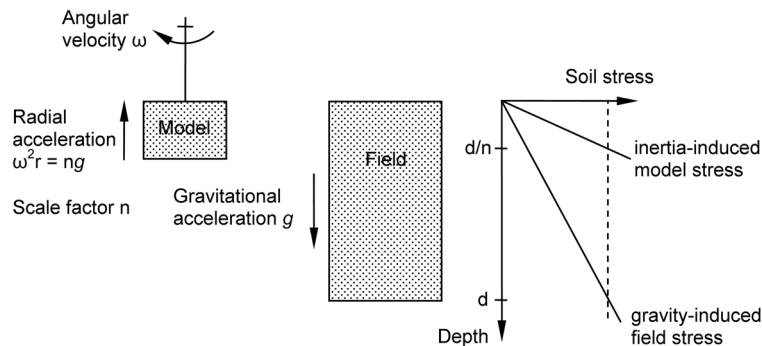


Fig. 4 Inertial stresses in a centrifuge model and corresponding stresses in a field model

equations and pavement design techniques, which could predict soil failure and rutting respectively are, in reality, difficult to apply due to the high flexibility and shallow section of the roadway.

A study of the complex interactions between vehicle tyres or tracks, flexible roadways and soil necessitates either field testing or the use of appropriately scaled physical modelling techniques. An advantage of reduced scale modelling is the greater control that may be exercised over loading and drainage boundaries and also over the recent stress history of the soil sample used as this is known to influence its constitutive behaviour. If drainage is controlled and pore water pressures known, then effective stresses in the soil may be established, thereby eliminating a significant uncertainty inherent to field testing (Muir Wood 2004).

The use of an appropriately scaled model in a geotechnical centrifuge is a well-established and convenient physical modelling technique that eliminates problems encountered in small-scale laboratory tests conducted at low stress levels. These relate to the stress level dependence of the mechanical properties of soils e.g. the applied stresses in reduced scale 1 g tests involving clays can be very small in relation to its undrained shear strength; in sands, the effects of dilation may be exaggerated. However, this is overcome by imposing an elevated gravitational field on a 1: n scale model by rotating the model at a constant angular velocity sufficient to impose an acceleration of n times gravity (g). Therefore, in a 1: n scale centrifuge model, whilst all linear dimensions are reduced by a factor of n , soil stresses and pore water pressures at all depths in the model are equal to their corresponding field scale values (Fig. 4). Due to the modelling convenience and requirements of similitude, research laboratories are increasingly using large scale geotechnical centrifuge modelling facilities such as beam and drum centrifuges (ISSMGE 1998, UST 2009) that, over recent years has led to the development of ever more sophisticated testing techniques and novel instrumentation. White (2008) provides a useful summary of recent developments in scaled physical modelling techniques involving geotechnical centrifuges.

This paper reports the application of centrifuge modelling techniques to impose rolling tyre loads on an aluminium roadway placed on a soft soil. The observed mechanisms that lead to roadway rutting are discussed. The influence of the articulated joints on roadway performance is demonstrated by comparing the results of rolling tyre loads imposed on jointed and non-jointed roadways. Simple elastic analysis solutions, calibrated by the centrifuge test results, are used to estimate contact stresses between the roadway and soil and to highlight the importance of roadway longitudinal flexural stiffness on its overall performance.

2. Centrifuge modelling procedure

The field scale roadway modelled in the centrifuge tests comprised a heavy duty aluminium roadway system (designated Class 60 trackway as it is designed to nominally support 60 tonne wheeled vehicles) 4.6 m wide that allows the passage of a 2.6 m wide heavy goods vehicle (HGV) with 1 m clearance on both sides. It is formed from 4.6 m long aluminium alloy panels with a corrugated section (Fig. 2) that maximises the transverse flexural stiffness to minimize rutting of the underlying soil. Articulating joints connect the panels to form a continuous roadway and which allow the roadway to be rolled on and off spools.

All centrifuge model tests were undertaken at a scale of 1:38, resulting in 120 mm wide model Class 60 roadway. Aluminium plate 0.6 mm thick provided the model-scale equivalent transverse flexural stiffness of the Class 60 trackway. The corrugations were too intricate to model at this scale and therefore the model roadway possessed the same transverse and longitudinal flexural stiffness. The tests were conducted at the London Geotechnical Centre using an Acutronic 661 geotechnical centrifuge incorporating a swinging platform which carries the model strongbox in which all models are contained. In flight, the surface of the platform will be vertical, rotating about a vertical axis in a circle of radius 1.8 m. The centrifuge is rated as a 40 g-tonne machine being capable of supporting a maximum payload of 400 kg at 100 g. A counterweight system is used to balance the model on the swinging arm. The principal design considerations and the specification of the Acutronic 661 machine are given by Schofield and Taylor (1988).

Both jointed and non-jointed roadways were tested in the centrifuge model. The jointed roadway comprised 5.5 mm wide panels formed from aluminium plates connected using a 30 μ m adhesive aluminium foil tape, as shown in a deformed post-test state in Fig. 5. A gap of 0.2 mm between each panel allowed free rotation/articulation between panels. The non-jointed version comprising a continuous 120 mm wide sheet of the aluminium plate was used to model the roadway in what may be considered a plane strain sense and allowed a comparison between the performance of the jointed (rollable) and a non-jointed roadway. The difference in performance between these two roadway models subsequently highlighted the influence of the articulated joints on roadway performance. Laboratory load-deflection tests on both model roadway types showed the jointed roadway to have a transverse flexural stiffness only 2% lower than that of the non-jointed roadway,

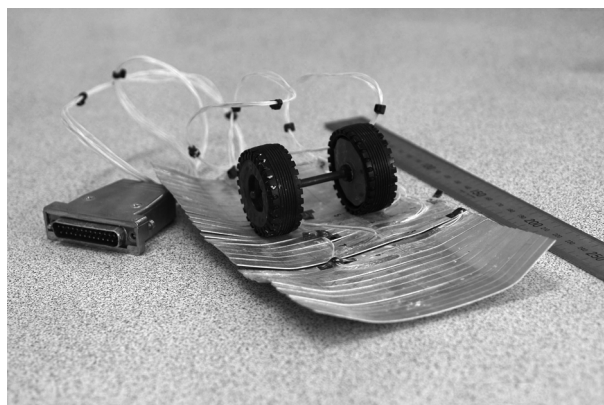


Fig. 5 Deformed jointed model roadway (post-test) showing strain gauges and model axle

so a significantly inferior performance of the jointed roadway could not be attributed to its lower flexural stiffness alone.

All soil preparation processes and tests were conducted in a model strongbox of plan dimensions 550 mm × 200 mm. The strongbox was fabricated from stiffened aluminium plates to ensure plane strain conditions i.e. deformations on the plane of loading only. A soft Speswhite kaolin clay sample was formed for each test by placing a kaolin slurry (95% moisture content) into the strongbox then transferring the strongbox to a consolidation press where the kaolin was one-dimensionally consolidated to a vertical effective stress of 106 kPa over a period of approximately two weeks. Kaolin clay is regularly used in centrifuge testing as its mechanical properties and constitutive behaviour are well characterised (e.g. Al-Tabbaa 1987) and its relatively high permeability ensures more rapid re-consolidation as initial conditions are established after spinning up the centrifuge.

This sample preparation process was similar for all tests and produced a soft clay with an average undrained shear strength (c_u) near the surface of 18 kPa (measured by triaxial compression tests). This is equivalent to a California Bearing Ratio (CBR) of about 1-2%. A soft clay such as this would have sufficient strength to support trafficking by a small dozer with wide tracks (Farrar and Daley 1975) but would necessitate the deployment of a temporary roadway to allow truck or multi-vehicle movements.

The strongbox containing the consolidated soil sample was removed from the consolidation press and the apparatus assembled as shown in Fig. 6 prior to placing onto the centrifuge swinging platform. The roadway was positioned on the soil surface in the centre of the model (Fig. 7) such that it ran longitudinally across the width of the strongbox. This formed a 7.6 m run of roadway at field scale. The clearances between the model roadway and the strongbox walls was 215 mm transversely and 305 mm vertically (Fig. 7: field dimensions are shown in brackets) ensuring end-effects were eliminated.

To apply tyre loads, two 44 mm diameter, 12 mm wide rubber “robotic” wheels with a total track width of 66 mm (thereby simulating typical truck tyre sizes and track widths) were connected to a 4 mm diameter steel axle. This was driven longitudinally along the roadway using steel forks that slotted over the axle and which imposed negligible vertical load during trafficking (Fig. 8). The

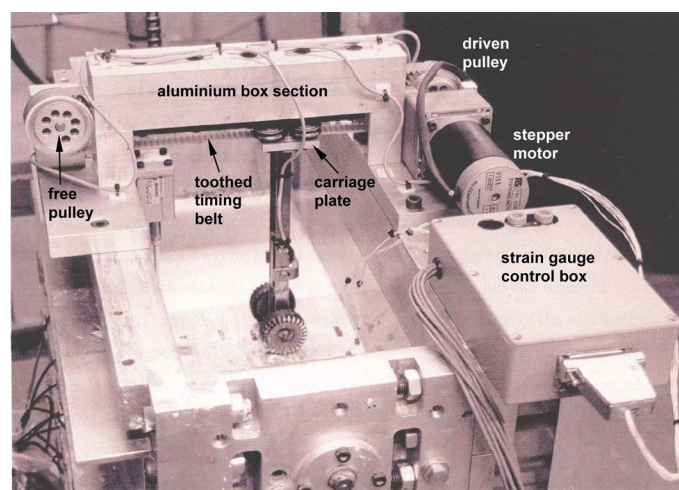


Fig. 6 Assembled centrifuge model showing axle driving apparatus fitted to strongbox

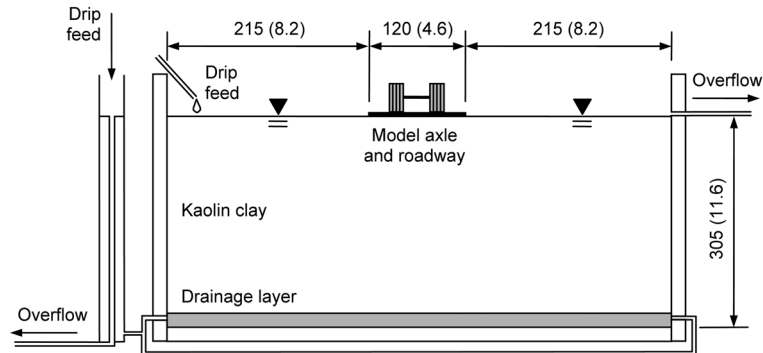


Fig. 7 Schematic cross-section of centrifuge model, showing geometry and drainage arrangement. Dimensions are in mm at model scale; figures in brackets correspond to metres at field scale

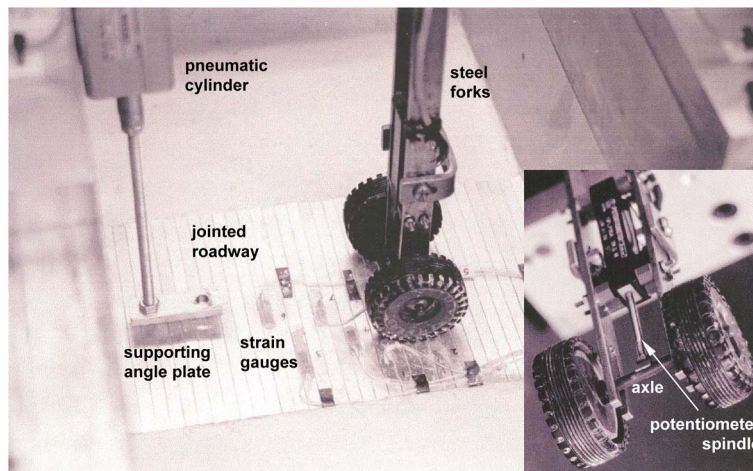


Fig. 8 Jointed roadway on soil surface, axle and driving forks in centrifuge strongbox

forks were suspended from a carriage plate that slid back and forth across the track via a linear slide bearing arrangement. The slide was supported from an aluminium box section spanning the full width of the strongbox. The carriage plate was driven by a hybrid stepper motor via a toothed timing belt and pulleys, all mounted onto the strongbox as shown in Fig. 6. A limit switch mounted at each end of the bridge allowed the drive direction to be reversed when activated by the carriage plate at the end of its travel. A counter timer on an A/D card recorded the number of trafficking cycles. Once set, the axle would continue to drive back and forth with no input from the user, until the motor control voltage was reduced to zero. The axle driving system proved very effective and no significant problems were encountered.

The axle was constrained to a travelling length of 130 mm (Fig. 9), or 4.9 m at field scale, by the strongbox geometry. Each traverse took 2.7 s to complete, corresponding to an axle speed of 0.05 m/s at both field and model scale (scale factor for velocity is 1:1). This is slower than normal vehicle speeds but since frequency is scaled by n , the model vehicle was traversing 9 panels per second of the jointed roadway (0.25 panels per second at field scale) and faster speeds risked

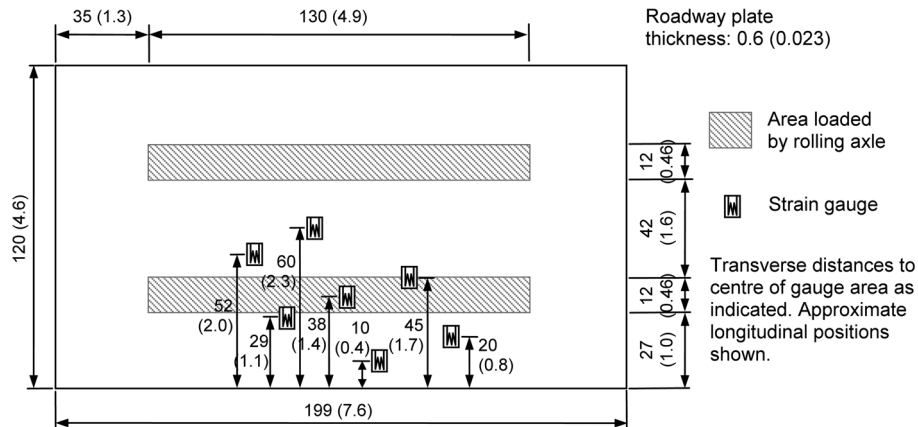


Fig. 9 Model roadway, showing strain gauge locations and area loaded by the rolling axle. Dimensions are in mm at model scale; figures in brackets correspond to metres at field scale

harming the jointed roadway. One effect of the slow speed may have been exaggerated consolidation of the clay under the axle load, particularly since consolidation time is scaled in the model at $1/n^2$. However, no significant consolidation was apparent from the roadway deformation as confirmed by moisture content measurements derived from samples obtained immediately after each test.

The axle load was 5 tonnes at field scale which is equivalent to 0.12 standard axles in pavement design, e.g. Croney and Croney (1991), and was applied simply by the enhanced self-weight of the axle under g , thereby ensuring the load was constant throughout the test, regardless of roadway deformations. Lead weights were fixed inside each rubber wheel to bring their weight up to 2.5 tonnes each at field scale. Care was taken to ensure each wheel had the same mass and that each wheel was balanced so that they rotated smoothly.

The average ground pressure imposed by the axle was estimated by coating each tyre tread with black ink and driving the tyres across white paper. Under its enhanced self-weight, the tyre imprints provided a typical contact area and an average ground pressure of 420 kPa was determined at both field and model scale. This value is typical of a light truck tyre indicating that the model axle/tyre system accurately replicated field axle loading conditions.

In Test NJR (non-jointed roadway) and Test JR (jointed roadway), the rolling axle was driven up and down the roadway system until either deformations reached such a level that hindered the progress of the rolling axle or a significant number of passes had been completed.

In all tests, pore water pressures were measured using Druck PDCR81 miniature transducers. These were installed at the plan centreline of the strongbox within the clay via a hole augered into the soil sample from the strongbox backplate and then backfilled with clay slurry at the locations shown in Fig. 10. The depth was limited to not less than 0.95 m at field scale to avoid deformation of the clay beneath the roadway. As well as monitoring excess pore pressures caused by the axle load, these transducers were also used to confirm the establishment of equilibrium conditions during the initial re-consolidation stage of each centrifuge test. During re-consolidation and throughout each test, water was supplied to the model by a drip feed to the clay surface, and a surface drain ensured the model did not flood (Fig. 7). To supply water to the base drainage layer of sand at the correct hydrostatic pressure, a second drip feed was placed in a standpipe with an internal overflow set to the height of the soil surface. This ensured that the clay remained fully saturated throughout

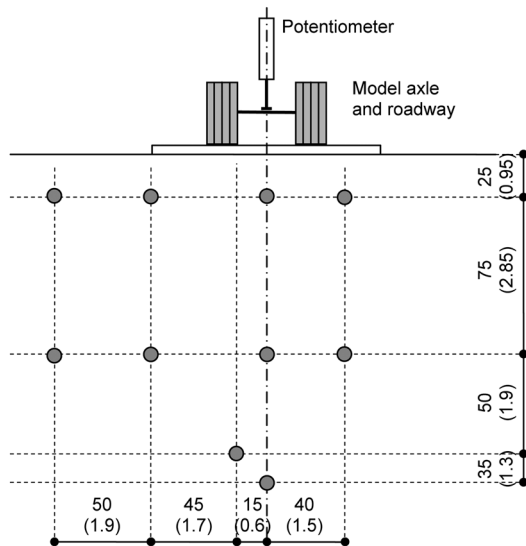


Fig. 10 Pore water pressure transducer and potentiometer locations in model. Dimensions are in mm at model scale; figures in brackets correspond to metres at field scale

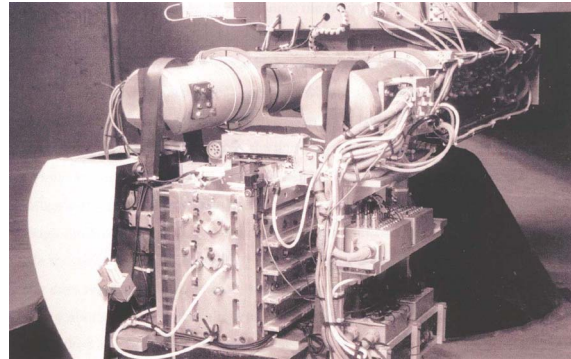


Fig. 11 Assembled centrifuge model strongbox mounted on the centrifuge swinging platform

the test.

The model axle was held clear of the roadway during the re-consolidation stage by an angle plate connected via a spindle to a pneumatic cylinder mounted to the strongbox wall (Fig. 8). On completion of the re-consolidation stage, the plate was lowered, allowing the axle to rest on the roadway ready to begin the trafficking cycles. A potentiometer (± 12.5 mm stroke) mounted between the driving forks with its spindle resting on the axle was used to measure vertical displacement of the rolling axle as it was driven over the roadway (Fig. 8).

Seven electrical resistance strain gauges were attached to the upper surface of each model roadway (Figs. 8 and 9) to allow transverse strain profiles during each test to be determined. An assembled model mounted on the centrifuge swinging platform is shown in Fig. 11. Only elastic strain measurement was possible using the electrical resistance strain gauges. Since these tests were conducted, there have been significant developments in optical strain measurement techniques for centrifuge modelling applications enabling both elastic and plastic deformations to be measured (White *et al.* 2003). These techniques are now emerging into mainstream centrifuge testing applications.

Following one-dimensional sample preparation in the consolidation press the clay is normally consolidated and the vertical effective stress is uniform throughout the sample. In the centrifuge however, the vertical stress profile caused by the enhanced self-weight of the clay will increase with depth from a value of zero at the surface. Therefore the clay near the surface becomes over-consolidated and, due to this stress history, will soften on yielding. Therefore, higher moisture contents will be expected where shearing of the clay occurs. To detect this, at the end of each centrifuge test and on spinning down, soil samples were taken from key locations to determine changes in moisture content.

3. Results and discussion

By applying appropriate scale factors to the centrifuge test data, equivalent field scale results were determined for a 4 tonne axle load on temporary roadway systems on soft clay. Linear dimensions in the model were scaled by a factor of n ($n = 38$ in both tests), forces by n^2 and mass by n^3 while material strength and stiffness values, velocity, stress and strain are identical in both the centrifuge model and at field scale. The results and analysis of the centrifuge tests are presented at field scale, unless otherwise specified. A full description of geotechnical centrifuge testing and scale factors is given by Schofield (1980).

3.1 Centrifuge Test NJR: rolling axle on non-jointed roadway

In Test NJR, the model axle with enhanced self-weight was allowed to pass over the non-jointed roadway in excess of 2000 times. Maximum axle settlements of 10 mm were recorded including an immediate 7 mm settlement at the start of the test. There was no significant accumulation of roadway deflection with successive passes and the non-jointed roadway performed effectively as a plate.

The recorded strains derived from electrical strain gauge output were less than 0.0008, well below the 0.002 value at which the aluminium starts to yield. The maximum excess pore water pressure was +7.5 kPa above hydrostatic and recorded in the shallowest transducer (0.95 m depth below the roadway). Since the shallowest transducer recorded the greatest change in pore water pressure, it is possible that higher pore water pressures occurred at depths less than 0.95 m.

3.2 Centrifuge Test JR: rolling axle on jointed roadway

In Test JR, the accumulation of roadway deflection contrasts markedly with that observed in Test NJR. Fig. 12 shows that after only 80 model axle passes, the jointed roadway settled 95 mm. Observation of the test via in-flight video showed that after only 2 axle passes, a clay slurry was visible between the roadway joints. After 6 axle passes, clay slurry was forced up onto the edges of the roadway and after 29 passes, slurry covered the entire roadway.

The accumulation of roadway deflection with successive axle passes matched field observations. Butterfield and Georgiadis (1980a) using a 1 *g* model landing mat panel subject to cyclic vertical loading at bearing pressures close to the bearing capacity of the soil, observed that the accumulation of deflections slowed to a constant oscillation and only increased by imposing a higher load amplitude. Fig. 12 shows the measured axial settlements with the number of axle passes plotted on a logarithmic scale in order to foreshorten the NJR trace and facilitate comparison with the JR trace. Plotted on a linear scale, the accumulation of permanent deflections is approximately linear and, in contrast to the findings of Butterfield and Georgiadis (1980a), did not reach a constant oscillation. This difference may have resulted from the pumping action of the rocking roadway panels that drove the slurry aside to expose intact clay after each pass that in turn further degraded to a slurry allowing continuous deformation of the roadway – an effect that could not be simulated by model tests on single panels.

The strain gauge data indicates that the jointed roadway deformed into a characteristic rutted profile (Fig. 13). However, only elastic strains were recorded and no permanent transverse roadway deflection occurred. This was due to the reversing motion of the axle: once the soil shear strength

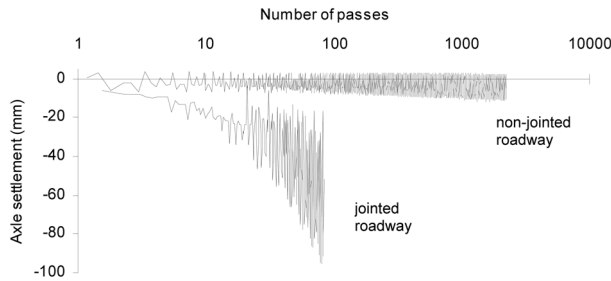


Fig. 12 Comparison of axle settlements on non-jointed and jointed roadway (Tests NJR and JR)

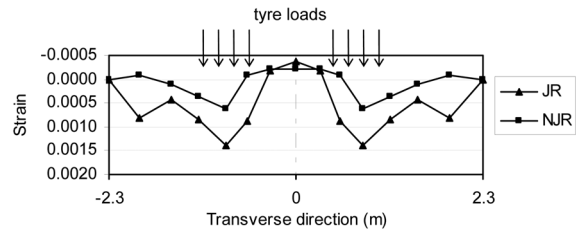


Fig. 13 Maximum transverse strain profiles recorded in Tests JR and NJR

had fully degraded to the point where a slurry was formed, rather than being forced to the sides of the roadway, the slurry beneath the roadway was driven to each end of the trackway with each axle motion. This created a deep trough in the longitudinal direction (pictured in Fig. 14 post-test) and accounts for the cyclic axle settlement profile shown in Fig. 12. Had it been possible to test a longer length of trackway within the strongbox, or perhaps continuous travel, as may be achievable in a drum centrifuge, it is likely that the clay slurry would have been forced out to the sides leading to permanent roadway deformations resembling the characteristic rutted profile typically observed in the field.

The average moisture content of the clay slurry sampled from immediately beneath and around the roadway was 56.1%, compared with 49.1% for intact clay 115 mm to 150 mm below the roadway. Assuming saturation of the clay, this corresponds with a 14% volume increase of the clay slurry and is indicative of softening of the over-consolidated clay at the surface resulting from shear failure.

A maximum excess pore water pressure of only 2 kPa was recorded in the shallowest transducer at 0.95 m depth, significantly lower than the 7.5 kPa recorded at the same depth below non-jointed roadway in Test NJR. This suggests that contact stresses beneath the jointed roadway were concentrated nearer the surface than beneath the non-jointed roadway, in areas where no pore pressure transducers could be installed. Clearly, the articulated joints were a major factor in the onset of roadway failure.

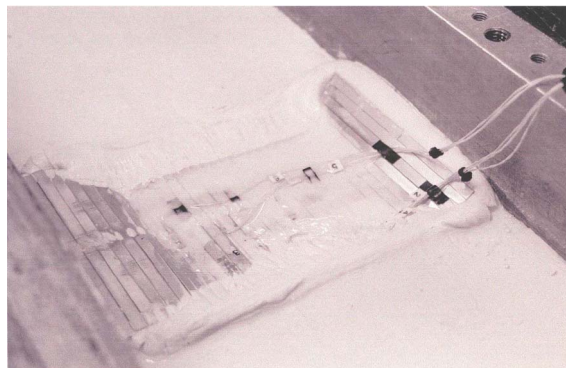


Fig. 14 Longitudinal trough formed in jointed roadway after Test JR

The rolling tyre load apparatus was successful and no significant problems were encountered. A disadvantage with the system was the short length of travel of the axle and the need to reverse the axle continually. A larger scale factor n would increase the length of travel but the need to reverse the axle could theoretically be avoided altogether by using a drum centrifuge i.e. a continuous roadway. A similar system perhaps could be designed for a drum centrifuge to allow continuous radial travel of an axle along a soil surface formed on the outer wall of the drum. Also, due to the short travel length, only a single axle was modelled. It was considered that the effect of multi-axle vehicle trafficking may be accommodated by simply summing the number of axle passes.

4. Estimation of contact stress and influence of joints

A roadway provides a means of evenly distributing tyre and track forces to the soil below, such that the soil is able to support trafficking forces without excessive deformation. The contact stress between roadway and soil determines the degree of soil deformation, so an ideal roadway system would distribute applied loads over the maximum soil area in order to minimise contact stress. Therefore, contact stress becomes a good measure of the efficiency of a roadway.

Since any instrumentation placed between roadway and soil would unduly influence the interactions being studied, contact stresses could not be measured directly. However, prior to failure they can be estimated using elastic analysis solutions of flexible plates resting on an elastic half-space, using elastic properties calibrated by the centrifuge tests.

An approximate analysis of point-loaded plates in frictionless contact on an elastic half-space was presented by Selvadurai (1979) and was used to estimate the contact stresses between roadway and soil in the centrifuge models. The assumption of point loads and frictionless contact will result in a gross over-estimation of deflections and contact stresses in comparison to the centrifuge test conditions, however this method is employed to facilitate a general comparison of the contact stresses between the jointed and non-jointed roadways. Firstly, roadway deflections were calculated and compared to measured deflections to further verify the method. Young's modulus and Poisson's ratio for the aluminium were $E = 69 \text{ GN/m}^2$ and $\nu = 0.33$ respectively. These parameters were verified by load-deflection tests on the model roadway conducted in the laboratory, and each tyre load was represented by a 24 kN point load. Poisson's ratio for the clay was taken as 0.4 to reflect both its essentially undrained behaviour ($\nu = 0.5$) and some dissipation of excess pore pressures during the loading that resulted in a partially drained response ($\nu < 0.5$). Back-analyses of earlier plane strain centrifuge models (Lees *et al.* 2002), indicated $E = 1000 \text{ kPa}$ for the soft kaolin clay. While this gives a very low undrained Young's modulus to undrained shear strength ratio E_u/c_u of about 56 (typical values range between 40 and 3000, e.g. Simons and Menzies 2000), low ratios do occur with clays of high plasticity under high shear stress levels, which were present in the centrifuge tests described here. Furthermore, a scale factor of $1/n^2$ for consolidation events resulted in some consolidation and increased deflection during the loading, resulting in a slightly reduced apparent stiffness. The resulting transverse roadway deflection profile for non-jointed roadway is shown in Fig. 15 where Transverse Direction = 0 marks the roadway centreline and each 0.46 m wide applied bearing pressure was applied at $x = \pm 1.0 \text{ m}$. Despite the expected over-estimation of deflection due to the assumptions highlighted above, the maximum calculated settlement was 19.4 mm compared to the maximum measured axle settlement values in Test NJR which increased from about 7 mm after 10 passes to approximately 10 mm after 1000 passes.

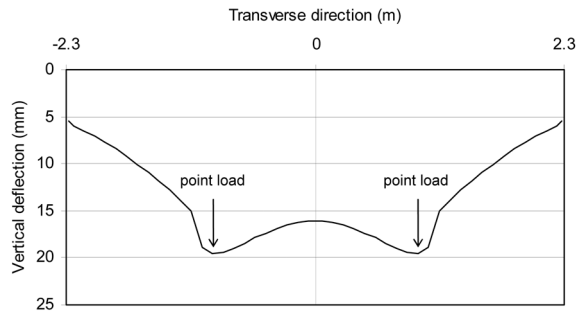


Fig. 15 Transverse deflected profile of unjointed roadway under concentrated wheel loads, from elastic analysis

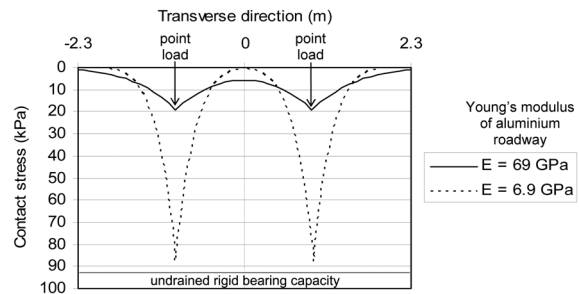


Fig. 16 Transverse profiles of estimated contact stress between unjointed roadway and clay under concentrated wheel loads

The estimated contact stress profile is shown in Fig. 16 under the same conditions, for the non-jointed roadway ($E = 69 \text{ GN/m}^2$). Undrained bearing capacity failure of a rigid strip footing occurs at a soil contact stress of $(\Pi + 2)c_u$, where c_u is the undrained shear strength. In the model clay, this value is 92.5 kPa (also plotted on Fig. 16), although in partially drained conditions this value would increase. Despite probable over-estimation, the maximum contact stress is well below that necessary to induce a rigid bearing capacity failure. This explains the non-accumulation of roadway deflection in Test NJR and is similar to that observed by Butterfield and Georgiadis (1980a) in cyclic load testing of model landing mat panels. For deflections to accumulate significantly on successive loadings, the amplitude of loading must be at 80% of the applied load at failure on first loading.

The influence of the articulated joints on contact stress can be estimated by reducing the Young's modulus of the roadway in the Selvadurai solutions. Also plotted in Fig. 16 is the estimated contact stress profile for a roadway with $E = 6.9 \text{ GN/m}^2$ (10% of normal value). This reduction allows the contact stresses to approach the rigid bearing capacity failure value. Since an articulated joint has virtually zero flexural stiffness in the longitudinal direction and with a nominal value of $E = 1000 \text{ kN/m}^2$ (same as the clay), the contact stress spikes to 34 MPa. The true maximum contact stress value beneath the jointed roadway probably lies somewhere between those obtained from $E = 6.9 \text{ GN/m}^2$ and $E = 1000 \text{ kN/m}^2$ and clearly would have resulted in immediate shallow-seated bearing capacity failure in these high contact stress zones.

Hemsley and Spence (1987) provide solutions for the transverse flexure of a strip foundation in frictionless contact with an elastic half-plane that further confirm the findings summarized above. They show that the contact stress between a strip foundation and the underlying homogeneous half-plane is directly related to the slope of the foundation in flexure. In Test NJR, the strain gauge data and observation of the in-flight video indicated that flexure of the non-jointed roadway, and hence its slope, under the tyre loads was small and therefore contact stresses were low. In Test JR, a rocking action of the roadway panels was observed creating steep slopes in the jointed roadway as the tyres rolled across each joint. Contact stresses must therefore have been high beneath each joint. However, the strain gauge data indicated that its deflected slope in the transverse direction was minimal (maximum recorded strain in first 20 passes was 0.0007), suggesting that contact stresses in the transverse direction were more evenly and better distributed.

The model landing mat load tests performed by Butterfield & Georgiadis (1980a) all involved concentric loadings, resulting in transverse bending but zero rotation of panels in the longitudinal sense. It is clear from the centrifuge test results that as tyre loads roll over articulated roadways,

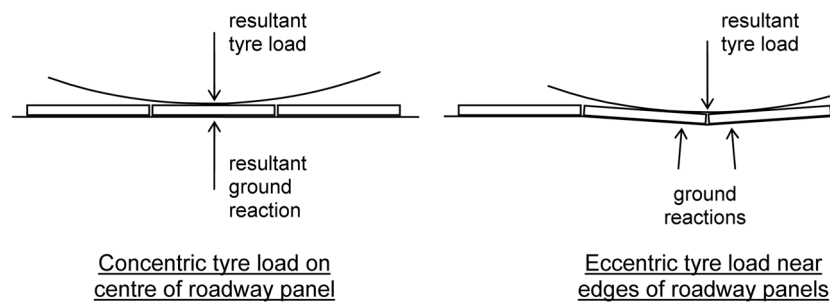


Fig. 17 Concentric and eccentric tyre loads on roadway panels

only for brief moments is the load applied concentrically to a panel and more usually the load is applied eccentrically (Fig. 17). The articulated joints allow the panels to rotate (in a repeated rocking motion as tyres roll over) into much steeper slopes than occur in non-jointed roadway, thereby creating high contact stresses directly beneath the edges, or articulated joints. It is clear, therefore, that restricting articulation of this joint during trafficking will reduce the contact stresses significantly. Once the roadway system has been deployed, a mechanical fixture that could effectively lock adjacent panels together to increase the panel width would enhance performance significantly.

Any modelling of a jointed roadway must consider flexure or rotation of panels in both the transverse and longitudinal directions. In physical terms this requires a model that contains jointed roadway and a method of load application that accurately simulates the rolling action of trafficking loads. In numerical terms this requires a versatile three-dimensional model, using finite element analysis for example, that can accommodate the complex loadings and interactions in jointed roadways and soil-structure interactions, e.g. Bagheripour *et al.* (2010).

The failure mechanism that accounts for the accumulation of roadway deflection in Test JR that matched field experience may be postulated as follows. Immediate, shallow-seated bearing capacity failures occurred due to high contact stresses under each loaded joint, which accounted for the immediate appearance of clay slurry and the rapid increase of axle settlement. The slurry was easily displaced by the rolling tyre loads to each end of travel of the axle and was constrained by the rigid boundaries imposed by the strongbox geometry. The roadway then settled into the resulting void.

5. Conclusions

A method of creating scaled rolling tyre loads along a surface in a centrifuge has been designed and successfully implemented. Using a single axle the results show that the effect of the axle load on the roadway is highly localised and the effect of multi-axle vehicle trafficking may be considered simply by summing the number of axle passes. The centrifuge tests demonstrated a marked difference in the performance of jointed (rollable) and non-jointed aluminium roadways subjected to rolling tyre loads. Significant roadway deflections failed to accumulate after 2000 axle passes on non-jointed roadway, while on roadway with articulated joints, deflections increased immediately and to such an extent that after less than 100 passes the rolling axle was impeded.

Elastic analysis solutions highlighted the influence of roadway flexural stiffness on contact

stresses between soil and roadway which in turn determines soil deformations and roadway performance. In contrast to previous work where the influence of joints were not considered, the articulated joints, with virtually zero flexural stiffness allowed very high contact stresses to develop leading to failure through the development of shallow-seated bearing failures under each loaded joint. Some means of resisting joint rotation once deployed would reduce the rocking action of the panels under trafficking, significantly reducing the maximum contact stress and thereby improving roadway performance.

Acknowledgements

The authors are grateful for the financial support provided by DERA (now QinetiQ). We would also like to thank Mr H. Skinner for his assistance in the development and preparation of the centrifuge apparatus.

References

- Al-Tabbaa, A. (1987), "Permeability & stress-strain response of speswhite kaolin", Ph.D. Dissertation, Univ. of Cambridge, UK.
- Arciszewski, B. and Wiedeck, H-N. (1987), "Rollable temporary roadway and apparatus for rolling up an installed temporary roadway", U. S. Patent 4681482, Jul.
- Bagheripour, M.H., Rahgozar, R. and Malekinejad, M. (2010), "Efficient analysis of SSI problems using infinite elements and wavelet theory", *Geomech. Eng.*, **2**(4), 229-252.
- Butterfield, R. and Georgiadis, M. (1980a), "The response of model, flexible landing mats to cyclic loading", *Proc. Int. Symp. on Soils Under Cyclic and Transient Loading*, Swansea, UK, 697-703.
- Butterfield, R. and Georgiadis, M. (1980b), "Cyclic plate bearing tests", *J. Terramech.*, **17**(3), 149-160.
- Cronej, D. and Cronej, P. (1991), *The design and performance of road pavements*, McGraw-Hill, London, UK.
- Davis, D. and Davis, R. (2004), "Temporary road bed", U. S. Patent 6575660, Mar.
- Farrar, D.M. and Daley, P. (1975), "The operation of earth moving plant on wet fill", Transport and Road Research Laboratory Report 688, Crowthorne, UK.
- Georgiadis, M. (1979), "Flexible landing mats on clay", Ph.D. thesis, Univ. of Southampton, UK.
- Glaza, G.K., Green, H.L. and White, D.W., (1994), "Accordion folding surfacing module", U.S. Patent 5275502, Jan.
- Hemsley, J.A. (1998), *Elastic analysis of raft foundations*, Thomas Telford, London, UK.
- Hemsley, J.A. and Spence, D.A. (1987), "Elastostatic plane strain flexure of a finite strip foundation in frictionless contact with a half-plane", *Proc. Instn. Civ. Engrs. (Structural Engineering Group)*, Part 2, **83**, 517-540.
- ISSMGE (1998), TC2 Geotechnical centrifuges worldwide, <http://geo.citg.tudelft.nl/allersma/tc2/cents.htm>, Sep 1998. Accessed May 25th 2010.
- Lees, A.S., Richards, D.J. and Skinner, H.P. (2002), "Development of cyclic loading and moving vehicle apparatus", *Physical modelling in geotechnics: ICPMG '02*, Balkema, Rotterdam, 427-432.
- Muir Wood, D. (2004), *Geotechnical modelling*, Spon Press, Abingdon, UK.
- Perry, R.E. and Myers, W.T. (1984), "Rapidly deployed assault vehicle surfacing or trackway system", U. S. Patent 4488833, Dec.
- Poulos, H.G. and Davis, E.H. (1974), *Elastic solutions for soil and rock mechanics*, John Wiley, Sydney, Australia.
- Schofield, A.N. (1980), "Cambridge geotechnical centrifuge operations. 20th Rankine Lecture", *Géotechnique*, **20**(2), 129-170.

- Schofield, A.N. and Taylor, R.N. (1988), "Development of standard geotechnical centrifuge operations", *Proc. Int. Conf. Centrifuge '88*, Balkema, Rotterdam, The Netherlands, 29-32.
- Selvadurai, A.P.S. (1979), *Elastic analysis of soil-foundation interaction*, Elsevier Scientific, Amsterdam, The Netherlands.
- Simons, N.E. and Menzies, B.K. (2000), *A Short course in foundation engineering*, 2nd edn., Thomas Telford, London.
- UST (2009), "Geotechnical centrifuges in the world", Hong Kong University of Science & Technology, <http://www.ust.hk/~webgcf/GCFCenter.html>, Accessed 17-Nov-2009.
- White, D.J., Take, W.A. and Bolton, M.D. (2003), "Soil deformation measurement using particle image velocimetry (PIV) and photogrammetry", *Géotechnique* **53**(7), 645-658
- White, D.J. (2008), "Contributions to Géotechnique 1948-2008: physical modelling", *Géotechnique*, **58**(5), 413-421.

CC